

Design and development of wideband gap-coupled slot rectangular microstrip array antenna

S N Mulgi, R B Konda, G M Pushpanjali, S K Satnoor & P V Hunagund
Department of PG Studies and Research in Applied Electronics, Gulbarga University
Gulbarga 585106 (Karnataka), India

Received 19 March 2007; revised 20 June 2007; accepted 27 June 2008

A novel design of four-element gap-coupled slot rectangular microstrip array antenna (FGSRMSA) is presented for broadband operation. The elements of antenna are fed using aperture coupled technique. From the experimental results it is seen that the antenna operates at single band of frequencies and shows broadside radiation characteristics. The overall impedance bandwidth is found to be 26.72 %, which is 1.114 times more than that of four-element gap-coupled rectangular microstrip array antenna (FGRMSA). This shows the effect of slots in enhancing impedance bandwidth of FGSRMSA. The slots in FGSRMSA also improve the antenna input impedance and increase the gain by 20.8% when compared to FGRMSA. Details of antenna designs are described and experimental results are discussed.

Keywords: Slot antenna, Aperture coupling, Array antenna, Microstrip antenna, Wideband antenna, Rectangular antenna

PACS No.: 84.40.Ba

1 Introduction

The microstrip antennas are very popular because of their low profile, conformal, low cost and ease in fabrication. They can be deployed for a wide variety of applications in microwave communication. However, microstrip antennas and their arrays inherently have narrow impedance bandwidth, which is one of their main drawbacks. Number of studies has been conducted on enhancement of impedance bandwidth of rectangular microstrip array antenna^{1,2}. In the year 2004, Chakraborty *et al.*³ have presented 4×4 rectangular aperture-coupled microstrip array antenna. They achieved nearly 11% of impedance bandwidth. But the proposed antenna is relatively compact in its size as it uses only four radiating and two parasitic elements. The obtained impedance bandwidth is 2.43 times more than found earlier³.

The antennas are sketched by using computer software Auto-CAD 2002 and fabricated on commonly available glass epoxy substrate material S_1 of thickness $h = 1.66$ mm and permittivity $\epsilon_r = 4.2$. The elements of four-element gap-coupled rectangular microstrip array antenna (FGRMSA) and four-element gap-coupled slot rectangular microstrip array antenna (FGSRMSA) are fed by using aperture-coupled technique. The dimension of slot placed at the center of radiating elements in the FGRMSA is

taken in terms of λ_0 , where λ_0 is free space wavelength in cm. The length L_s and width W_s of slot is taken as $\lambda_0/4$ and $\lambda_0/16$, respectively. This slot is considered as a wide slot, as its width is comparable to its length. The wide slot is selected because it is more effective in enhancing impedance bandwidth when compared to narrow slot⁴. The coupling slots are placed in the ground plane at the center with respect to the radiating elements, where the magnetic field of the radiating elements is maximum³. This is done to enhance coupling between the magnetic field of the radiating elements and the equivalent magnetic current near the slot.

2 Description of antenna geometry

Figure 1 shows the geometry of FGRMSA. The radiating and parasitic elements are etched on top surface of substrate S_1 . The corporate feed arrangement is etched on the bottom surface of the substrate S_2 having the same dielectric constant ϵ_r and thickness h as that of S_1 . The corporate feed arrangement consists of matching transformers, power dividers and microstrip bends (m) used for better impedance matching to the coupling slots. The coupling slots are placed on the top surface, which is the ground plane of the substrate S_2 exactly at the tip of 50- Ω microstrip feed line of corporate feed

arrangement. The radiating elements on the top surface of the substrate S_1 is energized through coupling slots placed on the top surface of the substrate S_2 . The substrate S_2 is placed below the substrate S_1 . This forms the aperture-coupled feeding technique⁵.

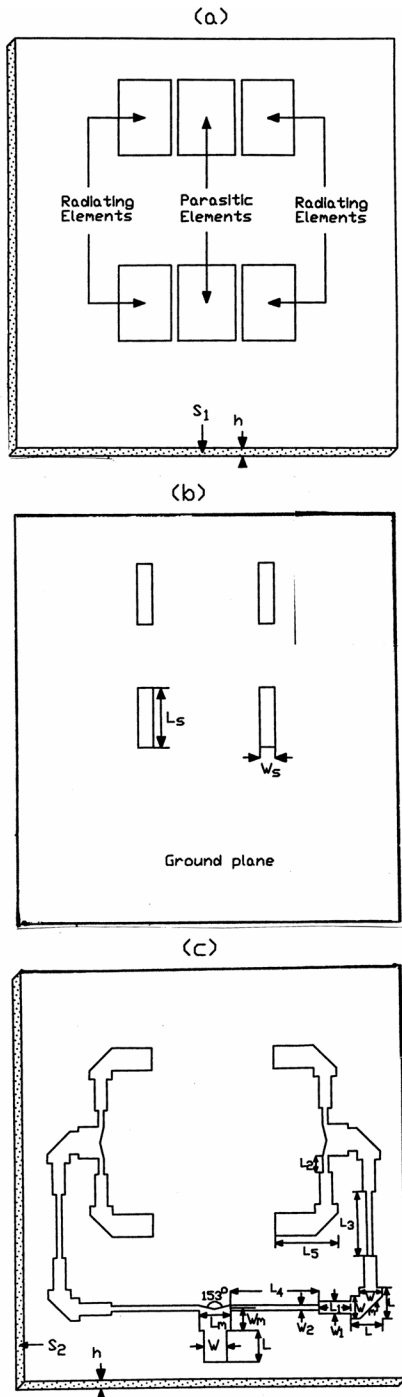


Fig. 1—Designed geometry of FGRMSA [(a) Array elements, (b) Slot array on ground plane and (c) Feed network]

The parasitic element is placed between the radiating elements along their widths, which forms the gap coupling. The distance between the parasitic and radiating element is taken⁶ as $S = 0.025 \lambda_g$, where λ_g is the operating wavelength⁴ in cm. The length of the parasitic element is adjusted in order to satisfy the distance condition $3\lambda_o/4$ between the two radiating elements⁷ from their center. Usually the spacing between the two radiating elements is kept at a distance of $\lambda_o/2$ for minimum side lobes. But in this case, it is difficult to accommodate corporate feed arrangement between the two radiating elements when the distance is $\lambda_o/2$. If this distance is increased, accordingly the feed line has to be extended, which increases radiation losses in the feed line. Hence, corporate feed arrangement is kept as small as possible by selecting spacing between two radiating elements to be $3\lambda_o/4$.

Figure 2 shows the geometry of FGSRMSA. The elements of Fig. 2 replace those of Fig. 1(a). In this geometry the slot is inserted at the center of radiating elements parallel to their width. The dimensions of radiating, parasitic, slot and corporate feed line network are as presented in Table 1.

3 Experimental results

The impedance bandwidth over return loss less than -10 dB for the proposed antennas is measured for X-band frequencies. The measurement is taken on Vector Network Analyzer. The variation of return loss versus frequency of FGRMSA and FGSRMSA is shown in Fig. 3. From this figure it is seen that the FGRMSA resonates for two bands of frequencies. From this graph the impedance bandwidth is determined by using the equation

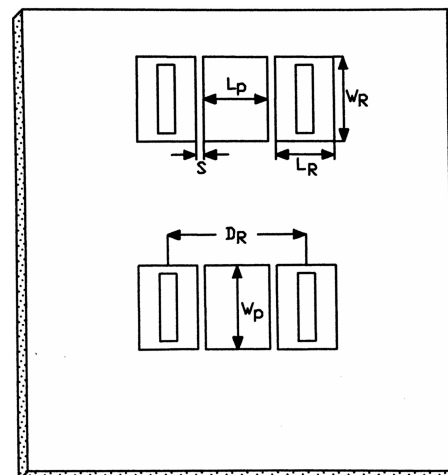


Fig. 2—Designed geometry of FGSRMSA

Table 1—Various dimensions of radiating and parasitic elements, slot and corporate feed line network

	Value, cm
(a) Patch dimensions	
Length of the radiating element (L_R)	0.71
Width of the radiating element (W_R)	0.99
Length of slot (L_s)	0.80
Width of Slot (W_s)	0.20
Length of the parasitic element (L_P)	0.80
Width of parasitic element (W_P)	0.99
Distance between the radiating & parasitic element (S)	0.04
Distance between two radiating elements (D_R)	1.61
Operating wave length (λ_g)	1.64
Free space wavelength (λ_0)	3.19
(b) Network dimensions	
Length of 50 Ω line (L)	0.41
Width of 50 Ω line (W)	0.30
Length of 50 Ω matching transformer (L_M)	0.41
Width of 50 Ω matching transformer (W_M)	0.30
Length of 70 Ω line (L_1)	0.41
Width of 70 Ω line (W_1)	0.16
Length of 100 Ω line (L_2)	0.21
Width of 100 Ω line (W_2)	0.07
Length of 100 Ω line (L_3)	0.83
Length of 100 Ω line (L_4)	1.15
Length of 50 Ω line (L_5)	0.52

$$BW = \left[\frac{(f_2 - f_1)}{f_c} \right] \times 100 \%$$

where, f_2 and f_1 are the higher and lower cut-off frequencies of the band respectively, when its return loss reaches -10 dB and f_c is the centre frequency of this band.

The experimental results show that the antenna operates at two wide bands of frequencies and the total impedance bandwidth ($BW_1 + BW_2$) is found to be 23.99%, i.e. 2.5 GHz. This impedance bandwidth is due to the combined resonance effect of parasitic elements and the coupling slots that couple energy from the feed line to the radiating elements. The coupling slot can be either resonant or non-resonant. If it is resonant, the current along the edges of the slot introduces an additional resonance⁸, which adds to the fundamental resonance of radiating element, causing enhancement in the impedance bandwidth.

Hence, from Fig. 3 it is seen that the enhancement in impedance bandwidth at (BW_1) and (BW_2) is due to resonance of radiating elements through coupling slots and resonance of parasitic elements near to the

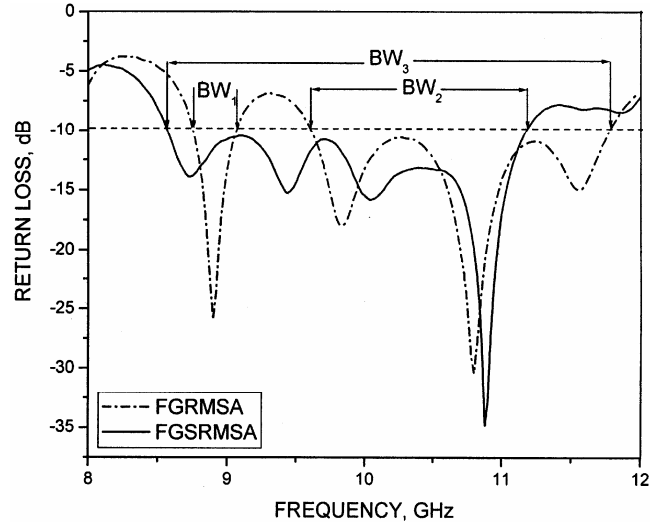


Fig. 3—Variation of return loss versus frequency of FGRMSA and FGSRMSA

radiating elements⁶. The maximum return loss achieved at (BW_1) and (BW_2) is -26 dB and -30 dB, respectively. Further from this figure it is seen that the FGSRMSA operates at one band of frequency and gives an impedance bandwidth (BW_3) of 26.72%, i.e. 2.64 GHz, which is 1.114 times more than that of FGRMSA and with a greater return loss of up to -33 dB. This enhancement of impedance bandwidth is due to the combined effect of radiating and parasitic elements as explained for FGRMSA, which acts as a primary resonator, and the slot in the radiating patches acts as secondary resonator⁸⁻¹⁰. The combined effect of these resonances causes merging of bandwidths BW_1 and BW_2 and hence gives only one bandwidth BW_3 , which is as shown in Fig. 3.

In order to calculate the gain, the power received (P_s) by the pyramidal horn antenna and the power received (P_t) by FGRMSA and FGSRMSA are measured independently at their resonant frequencies. With the help of these experimental data the gain of antenna under test (G_T) in dB is calculated using the formula

$$(G_T)_{dB} = (G_s)_{dB} + 10 \log (P_t/P_s)$$

where, G_s is the gain of pyramidal horn antenna. From this the gain of FGRMSA and FGSRMSA is found to be -13.11 dB and -10.38 dB, respectively. It is evident that the use of slots in the radiating elements in FGSRMSA increases the gain by 20.8%.

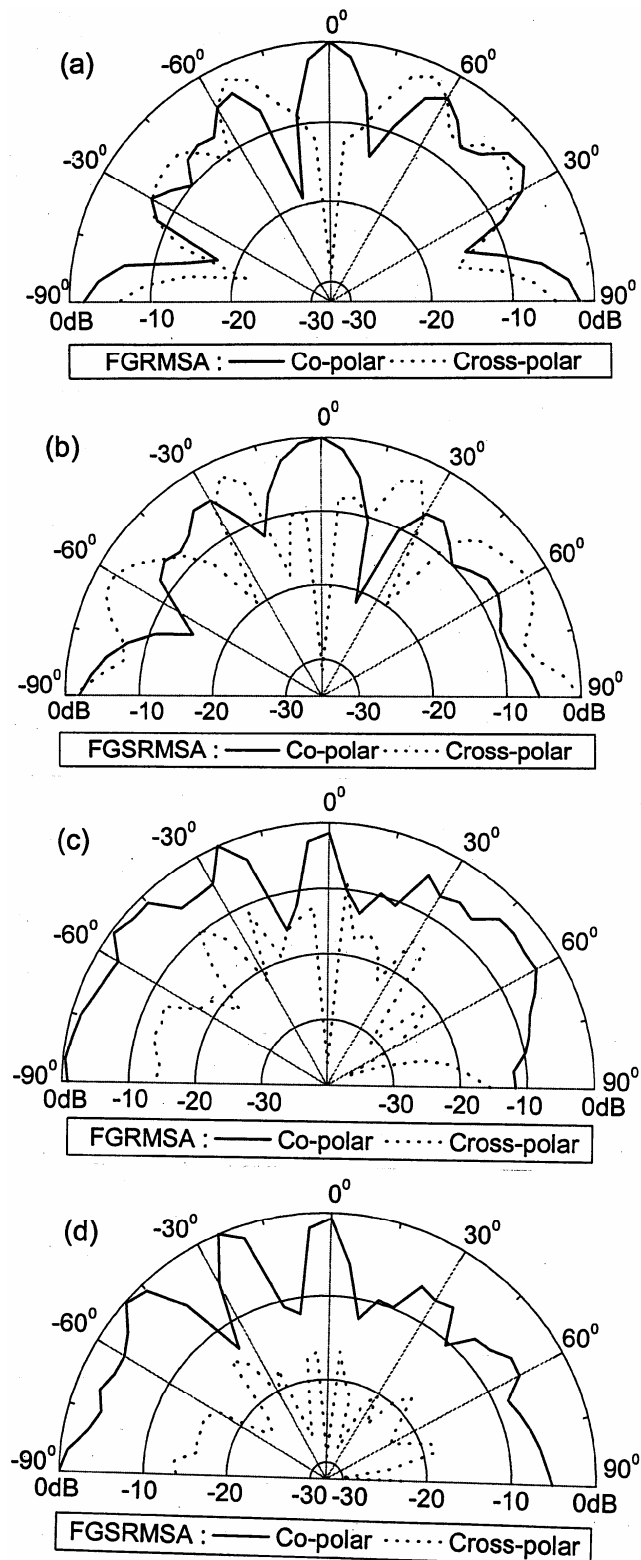


Fig. 4—Variation of relative power versus azimuth angle of (a) FGRMSA in H-Plane, (b) FGSRMSA in H-Plane, (c) FGRMSA in E-Plane and (d) FGSRMSA in E-Plane

The co-polar and cross-polar H- and E-plane radiation patterns of FGRMSA and FGSRMSA are measured in their operating band. The typical radiation patterns of these antennas are shown in Fig. 4[(a)-(d)]. From Figs 4(a) and (b), it is seen that H-plane radiation patterns are broad sided with side lobes and cross-polar levels are below -5 dB, indicating linear polarization of radiation¹¹ and pattern is uniform from their center axis. From Figs 4(c) and (d), it is found that the E-plane co-polar radiation patterns are having minimum side lobes and gives better broadside radiation pattern and the cross-polar levels are below -10 dB. This shows the merits of E-plane co-polar and cross-polar radiation patterns when compared to H-plane co-polar and cross-polar radiation patterns. Further from Figs 4(a) and (b), it is seen that the FGSRMSA gives wider beam-width as that of FGRMSA. The wider beam-width is because of insertion of slots in the radiating patches of FGSRMSA. However the FGSRMSA resonates with a greater return loss and hence gives more gain than that of FGRMSA, which is evident from Fig. 3. It is also observed that the input impedance of FGSRMSA is well matched in the operating band of frequencies.

4 Conclusion

The present study shows that the impedance bandwidth of FGSRMSA can be enhanced significantly by adding optimum slots in the radiating elements. The maximum impedance bandwidth of 26.72% is achieved in case of FGSRMSA at X-band frequencies (8-12 GHz). This impedance bandwidth is 1.114 times more than that of FGRMSA and 2.43 times more than the earlier result³ without changing broadside-radiating characteristics. This shows the effect of parasitic elements and slots for enhancing impedance bandwidth by using aperture-coupled feeding. The proposed method also improves the input impedance of antenna and increases the gain by 20.8% when compared to FGRMSA. Hence, these compact, wide band antennas are attractive for present-day scientific and industrial application in fields like mobile computing and communication³.

Acknowledgements

The authors would like to thank Department of Science & Technology (DST), New Delhi, for sanctioning Network Analyzer to this Department under FIST project. The authors also express there thanks to D Govind Rao, Scientist, Electronic and

Radar Development Establishment (LRDE), Bangalore, for providing measurement facilities and useful discussions.

References

- 1 Mestdagh Steven, De Raedt Walter & Guy A E Vandebosch, CPW-fed stacked microstrip antenna, *IEEE Trans Antennas Propag (USA)*, 52 (2004) 74.
- 2 Buerkle Amelia, Sarabandi Kamal & Mosallaei, Compact-slot and dielectric resonator antenna with dual-resonance, broadband characteristic, *IEEE Trans Antennas Propag (USA)*, 53 (2005) 1020.
- 3 Chakraborty Samik, Gupta Bhaskar & Poddar D R, Development of closed form design formulae for aperture coupled microstrip antenna, *J Sci Ind Res (India)*, 64 (2005) 482.
- 4 Bahl I J & Bhartia P, *Microstrip Antennas* (Artech House, New Delhi), 1981.
- 5 Pozar David M, Analysis of an infinite phased array of aperture coupled microstrip patches, *IEEE Trans Antennas Propag (USA)*, 37 (1989) 418.
- 6 Mulgi S N, Vani R M, Hunagund P V & Hadalgi P M, A compact broadband gap-coupled microstrip antenna, *Indian J Radio Space Phys*, 33 (2004) 139.
- 7 Constantine A Balanis, *Antenna Theory Analysis and Design* (John Wiley, New York), 1982.
- 8 Jeon-Sheon Row, Dual-frequency triangular planar inverted-F antenna, *IEEE Trans Antennas Propag (USA)*, 53AP (2005) 874.
- 9 Yang X H & Shafai L, Multifrequency operation technique for aperture coupled microstrip antenna, *Antennas & Propagation Society Int. Symp. AP-S Digest*, 20-24 (1994) 1198.
- 10 Rafi Gh Z & Shafai L, Wideband V-slotted diamond-shaped microstrip patch antenna, *Electron Lett (UK)*, (2004) 40.
- 11 Praveen Kumar A V & Mathew K T, Cylindrical dielectric resonator antenna with a coplanar parasitic conducting strip, *Proc APSYM-CUSAT 06*, (2006) 171.